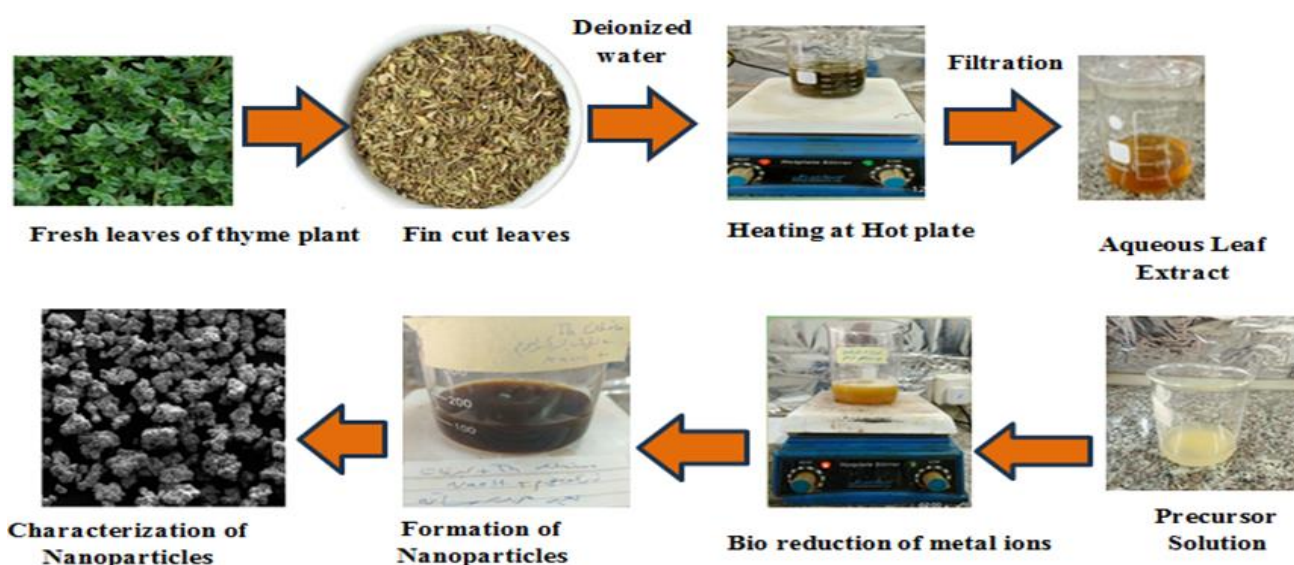


Green Synthesis, Characterization, Antimicrobial and Anticancer Studies of Zirconium Oxide Nanoparticles Using Thyme plant Extract

Wafaa Fayyad Tharp¹, Lekaa K. Abdul Kareem^{2*}

^{1,2} Departments of Chemistry, College of Education for Pure Sciences, Ibn Al-Haitham, University of Baghdad, Iraq

*For Corresponding author: Email address: likaa.k.a@ihcoedu.uobaghdad.edu.iq (L. K. A. Kareem)



Received 9 Jan 2024,
Revised 06 Feb 2024,
Accepted 07 Feb 2024

Citation: Tharp W. F., Abdul Kareem L. K. (2024) Preparation of nano-zirconium oxide and studying its testing against antioxidants, *Mor. J. Chem.*, 12(2), 643-656

Abstract: In this work we used the environmentally friendly method to prepared ZrO_2 nanoparticles utilizing the extract of Thyme plant. In basic medium and at pH 12, the ZrO_2 NPs was characterized by different techniques such as FTIR, ultraviolet visible, Atomic force microscope, Scanning Electron Microscopy, X-ray diffraction and Energy dispersive X-ray. The average crystalline size was calculated using the Debye Scherrer equation in value 7.65 nm. Atomic force microscope results showed the size values for ZrO_2 NPs were 45.11 nm, and there are several distortions due to the presence of some large sizes. Atomic force microscope results showed the typical size values for ZrO_2 NPs were 45.11 nm, and there are several distortions due to the presence of some large sizes, the results of SEM show that values size of particles ZrO_2 NPs was 18.70 nm, zirconium oxide nanoparticles are formed in small clusters. Antimicrobial activities have been studied of ZrO_2 NPs against one type of positive bacteria such as Bacillus, Klebsiella and Candida fungus in different concentrations, ZrO_2 NPs showed different effectiveness against these different types of antimicrobials. ZrO_2 NPs was studied to inhibit breast cancer cell line (MCF-7). The results showed a high ability of the ZrO_2 NPs to inhibit cancer cells.

Keywords: Anti-cancer, Environmentally friendly, Green Synthesis, Plant Extract, Zirconium oxide.

1. Introduction

As a result of the fact that nanotechnology empowers the production of advanced nanoparticles with individualized dimensions and configurations, it has garnered interest in a wide variety of scientific fields, such as physics, chemistry, biology, engineering, medicine, and materials science (Hameed and Abdulrahman, 2023; Herradi *et al.*, 2024; Azzaoui *et al.*, 2016). The creation of nanoparticles (NP) can be performed in a variety of ways; however, green approaches, which are less detrimental to the environment, more cost-effective, and give viable alternatives to physical and chemical procedures, are increasingly being prioritized within the industry. When utilized in chemical processes, they are not only expensive but also hazardous (Salem and Fouda, 2021; Salem *et al.*, 2022). Chemicals, additives, or both are utilized in order to achieve a more stable state of affairs. It is not uncommon for synthesis techniques to involve the utilization of solvents that are neither biodegradable nor polar. In addition, these operations usually involve the application of extreme temperatures and pressures (Balasooriya *et al.*, 2017; Azzaoui *et al.*, 2023; Aaddouz *et al.*, 2023). Through the utilization of a wide range of sources, including bacteria, fungus, algae, and plant extracts, biosynthesis offers an alternative method for the production of NP that does not need the use of hazardous chemicals. Plant extracts have become a widespread choice among these alternative sources due to the stability of the nanoparticles that are created, as well as the relative easiness, low cost, and absence of environmental damage that happens during the synthesis process (Ruaa *et al.*, 2021; Azzaoui *et al.*, 2014; El Hammari *et al.*, 2023). Preservative and buffering properties are provided by the plant extract in this particular instance. Several plant extracts, such as those of neem (*Azadirachta indica*), hibiscus (*Hibiscus rosa sinensis*), and Indian gooseberry (*Emblica officinalis*), amongst others, have been utilised in the process of synthesizing metal oxide nanoparticles (NPs). While this is the case, multiple discoveries have been made regarding the plant-mediated generation of ZrO₂ nanoparticles from a variety of sources, including *Euclea natalensis* (Al-Bahadili *et al.*, 2022; Errich *et al.*, 2021) pathogenic fungus *Fusarium solani* (Bukhari *et al.*, 2021), plant leave (Qiu *et al.*, 2020), Curcuma longa (Khan *et al.*, 2022), pomegranate peel (Singh and Singh, 2019) cinnamon (Karem and Ali, 2023; Tabaght *et al.*, 2021; Akartasse *et al.*, 2022; Jerdioui *et al.*, 2024) and so on. Research has been conducted on a wide variety of applications, such as adsorption, calculations of thermodynamic functions, the biological effectiveness of ZrO₂ Nano oxide, its toxicity, and antioxidants (Ebrahimian *et al.*, 2020; Hamdouch *et al.*, 2023; Diniz *et al.*, 2019; Jerdioui *et al.*, 2017; Meziane *et al.*, 2024).

Thymus vulgaris is a flowering plant of the family Lamiaceae commonly known as thyme, (Hosseinzadeh *et al.*, 2015). *Thymus vulgaris* was first known for its aromatic effects and then its analgesic and anti-inflammatory effects in various cutaneous diseases were proven (Alexa, Ersilia, *et al.*, 2018). It is also noticeable by its expectorant effect and its utility in gastrointestinal disorders. Because this plant belongs to the Lamiaceae family, both oil and thyme extract have a large number of hydroxyl groups, which is why they have a strong antioxidant effect. Two phenolic compounds namely thymol and carvacol are found in high concentrations in the essential oil of *Thymus vulgaris* (thyme) as also in the different species of *Thymus* (Al-Menhali, *et al.*, 2015). The Major Compounds of Thyme Plant was show in **Table 1**. The richness of *Thymus vulgaris* extract in various components containing aromatic rings, double and triple bonds as well as heteroatoms, permitted numerous applications in medical uses and protection of corrosion of metals in aggressive media (Maizia, *et al.* 2023; Gonzalez-Rodriguez *et al.* 2022; Horváth, *et al.* 2021; El Hajjaji *et al.* 2016).

The synthesis of metal nanoparticles (NPs) has provoked researchers' interest since they have diverse applications. Presently, the concept 'green synthesis' or 'plant-mediated synthesis' has been devised for the synthesis of NPs, which significantly contribute to the conservation of the environment

and reduces risk factors in humans and does not need a reducing agent or a stabilizer (Azadi, Minoo, *et al.* 2021).

In this research, we developed a method that yields ZrO₂ nanoparticles in a manner that is biologically friendly. Powder metallography, electron microscopy, atomic force microscopy, and electron density spectroscopy are some of the nanomaterial diagnostic methods that have been utilized in the process of characterizing Nano oxide. In addition, examinations into its antibacterial characteristics and the effect of Nano zirconium oxide on the MCF-7 cell line have been conducted as part of the research that has been conducted on its prospective applications.

2. Methodology

2.1 Materials and Methods

Acquiring specimens, we obtained the *Thyme vulgares* from a local source and employed zirconium sulfates were bought from Merck Germany, sodium hydroxide from Sigma Aldaraj America, and Deionized water from local markets.

2.2 Experiments: Preparation of Thyme Extract and ZrO₂ NPs

The same method in (Karem and Ali, 2023) was used to prepare Zirconium oxide NPs, dust has been removed from the *Thyme* by washing it with deionized water, and leave to dry. Following that, 200 ml of deionized water was mixed with 20 g of Thyme dried. The mixture was mixed and heated to 65 °C for 30 minutes on hot plate. The solution was put in the centrifuge it had been filtered. The green synthesis approach was used to produce NPs from the production of ZrO₂. Thus, 100 mL of, Zr(SO₄)₂ and 100 mL of extract from Thyme were added gradually, after adding 50 mL of (1 N) sodium hydroxide to the mixture one drop at a time, the pH (10–12). This resulted in a precipitate of yellow crystals that were cleaned with deionized water. Each step has been done with a centrifuge, then decantation. It was then baked for 5 hours and sintered at 600°C, producing a brown powder that contained zirconium oxide nanoparticles.

2.3. Antimicrobials study

In a nutrient medium known as Muller Hinton agar, which was used for *Bacillus*, *Klebsiella*, and *Candida* fungus, and potato dextrose agar, which was used for *Candida* fungus, antibiotics were used to determine the bactericidal properties of the prepared ZrO₂ nanoparticles. The concentrations of the ZrO₂ nanoparticles were as follows: 25%, 50%, and 100% mg/L in DMSO solvent medium (Ghani *et al.*, 2022; Al Jabbar *et al.*, 2020; Amer, 2022; Carreño *et al.*, 2021).

2.4. Cytotoxic Assays

The MTT assay was used to ascertain the activity of ZrO₂ NPs at different concentrations (15.625, 31.25, 62.5, 125, 250, and 500) µg/mL against MCF-7 cell lines on breast and the degree of cancer to which these different cells affect them by applying a calorimetric technique to diagnose the metabolic activity of the cell (Shvets *et al.*, 2019; Alsaheb, 2020).

2.5 Product characterisation

The compound was created and identified using a variety of spectroscopic and microscopic techniques and the devices, such as a magnetic stirrer, an electric oven type PC21-A, Batec, an electric centrifuge type PLC(80-1), and a sensitive electronic balance model (As 220C1) with a Phillips/Netherlands (PW1730) XRD diffraction type. The UV-visible tape measure, The FT-IR

sgimadzu Japan type spectroscopy (1800), and center of investigations in range 400–4000 cm^{-1} . The X-ray energy dispersion apparatus, SEM type FESEM-EDS Model, MIRAI III producer manufacturing nation of Czechia (EDX) and Atomic Force Microscopes AFM with model number EM10C-100Kv-Zeiss, Germany.

3. Results and Discussion

3.1 FT-IR analysis

FTIR spectrum of Thyme extract at range (4000-400) cm^{-1} show (Figure 1a). FTIR spectrum of ZrO_2 NPs at range (4000-400) cm^{-1} show the bands at (472.56 -862.48) cm^{-1} due to Zr and O bond in the ZrO_2 vibration stretching mode. The bands at (3203, 1556, 1371, 962) cm^{-1} were due to remaining active groups in the plant extract might be the cause of the other bands vibration stretching of O-H, C=C and C=O, respectively, (Figure 1b) (Mahdi & Karem, 2020; Aliyu, *et al.*, 2017; Abdalsahib & Karem, 2023). The collected and suggested chemical compounds of Thyme are presented in Table 1, according to the literature (Proks, *et al.*, 2019).

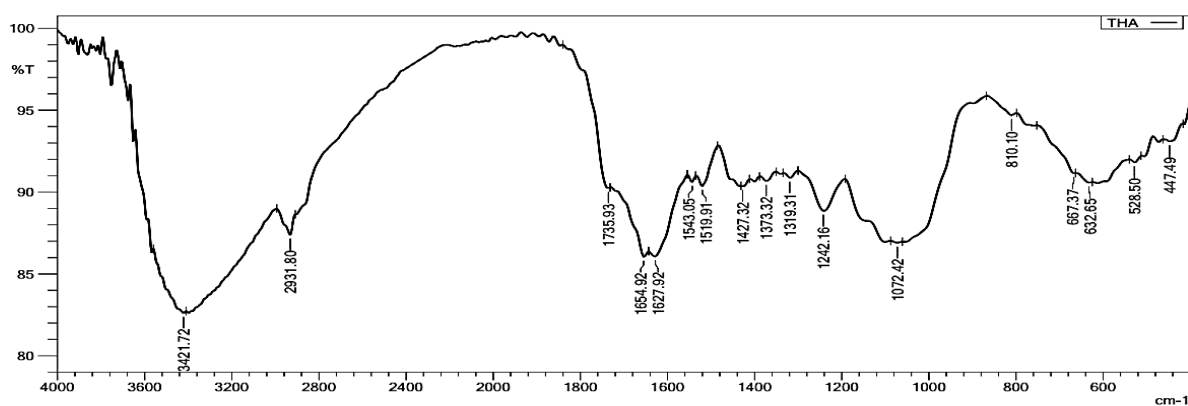


Figure 1a: The FTIR of thyme plant extract

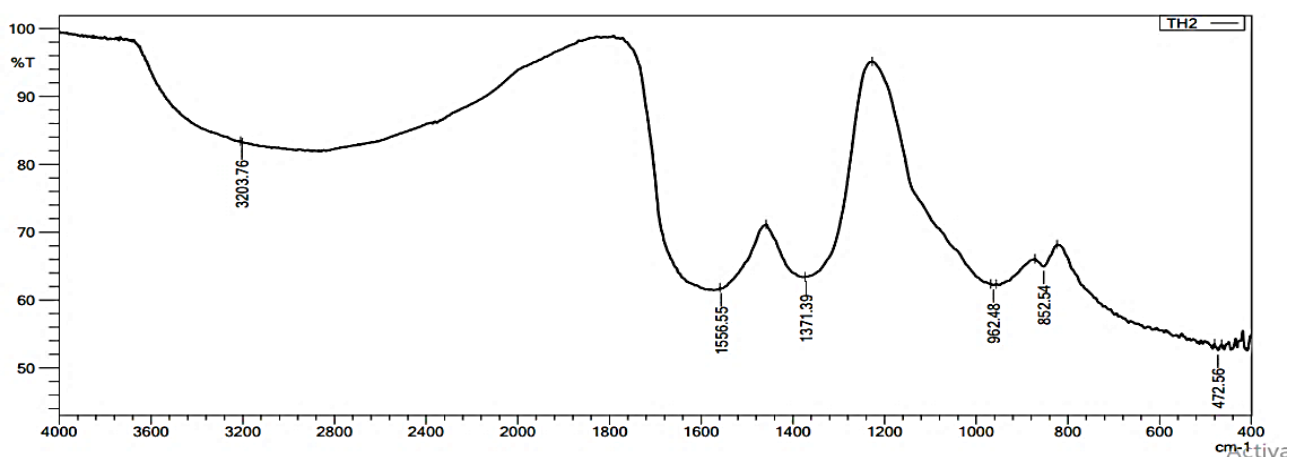
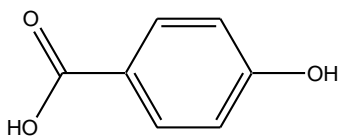
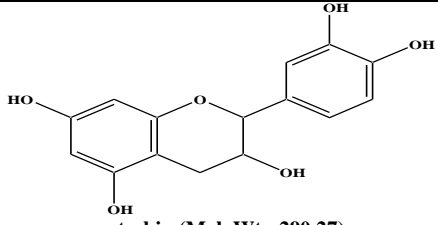
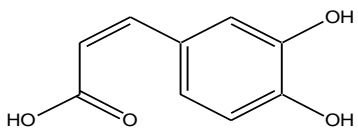
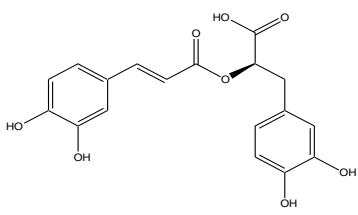
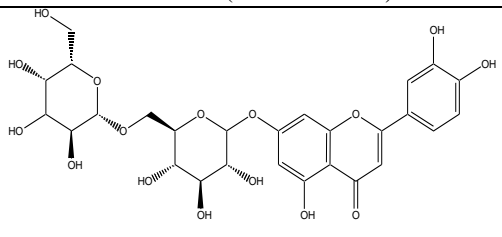
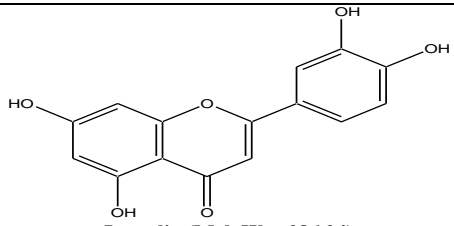
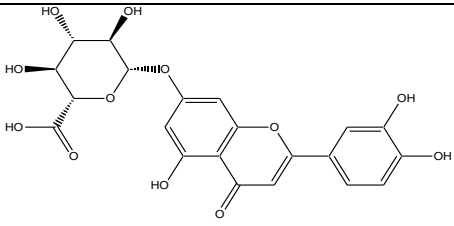
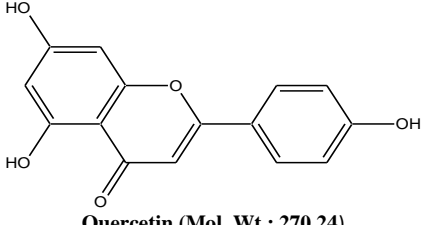
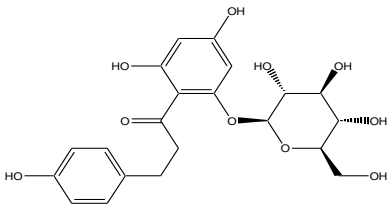
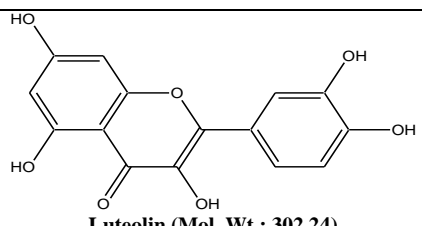
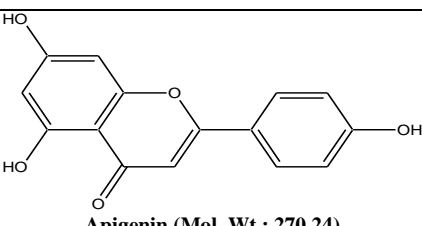


Figure 1b. FT-IR spectrum for ZrO_2 NPs

3.2 UV-Visible analysis

UV-Vis absorption spectrum of ZrO_2 nanoparticles is displayed. The absorption peak of this spectrum can be seen at 470.0 nm, which is caused by the transition holes process that occurs between Zr and O. The energy gap was calculated based on; $E_g = 1240 / \lambda$ which is to be 2.638 eV. For ZrO_2 NPs (Figure 2) (Subramanian *et al.*, 2019)

Table 1: The Major Compounds of Thyme Plant

 Thyme Plant Aqueous Extract	 p-hydroxybenzoic acid (Mol. Wt.: 138.12)
 catechin (Mol. Wt.: 290.27)	 Caffeic acid (Mol. Wt.: 180.16)
 Rosmarinic acid (Mol. Wt.: 360.31)	 Eriocitrin (Mol. Wt.: 610.52)
 Luteolin (Mol. Wt.: 286.24)	 Phloridzin (Mol. Wt.: 462.36)
 Quercetin (Mol. Wt.: 270.24)	 Apigenin-7-O-glucoside (Mol. Wt.: 436.41)
 Luteolin (Mol. Wt.: 302.24)	 Apigenin (Mol. Wt.: 270.24)

3.3 AFM analysis

The topography of the Earth, which is a representation of the elevation and structure of the surface, can be determined through the use of atomic force microscopy. Digital images that enable quantitative assessments of surface properties are referred to as this technology. Instances of this technology include image analysis from a variety of viewpoints, as well as three-dimensional simulation technologies (Al-Saadi and Kamil, 2023), 3D AFM images and detail distribution of ZrO₂ NPs synthesized by green methods, the images are shown in **Figures 3, 4**. It is imperative to see that

typical values size of ZrO₂ NPs was 45.11 nm, and there are several distortions of the presence of some large sizes.

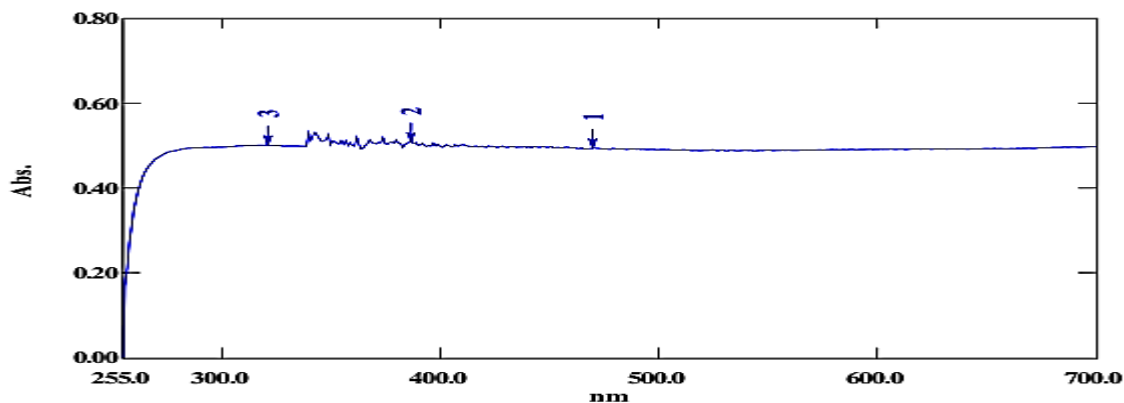


Figure 2. UV visible spectrum of ZrO₂ NPs

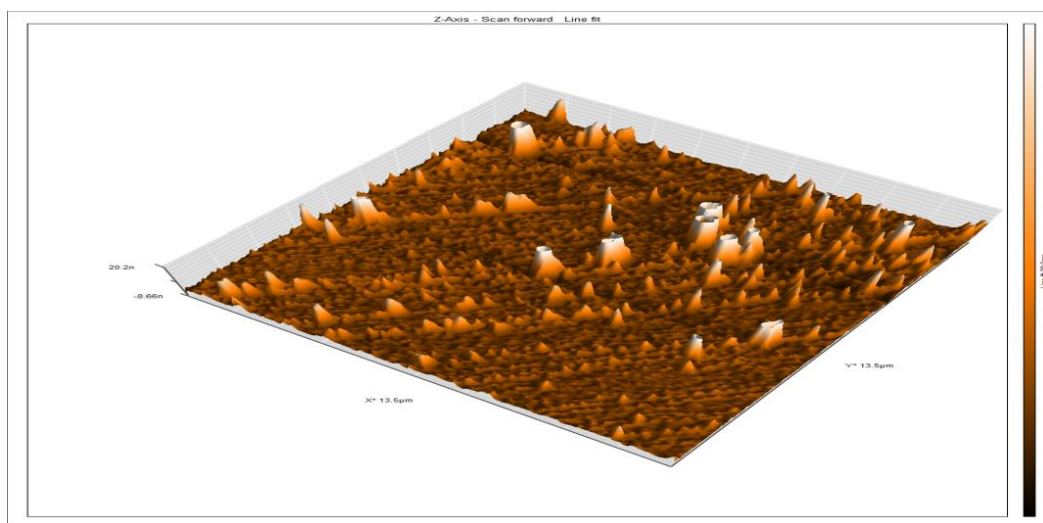


Figure 3. The AFM -3D dimensional of ZrO₂ NPs.

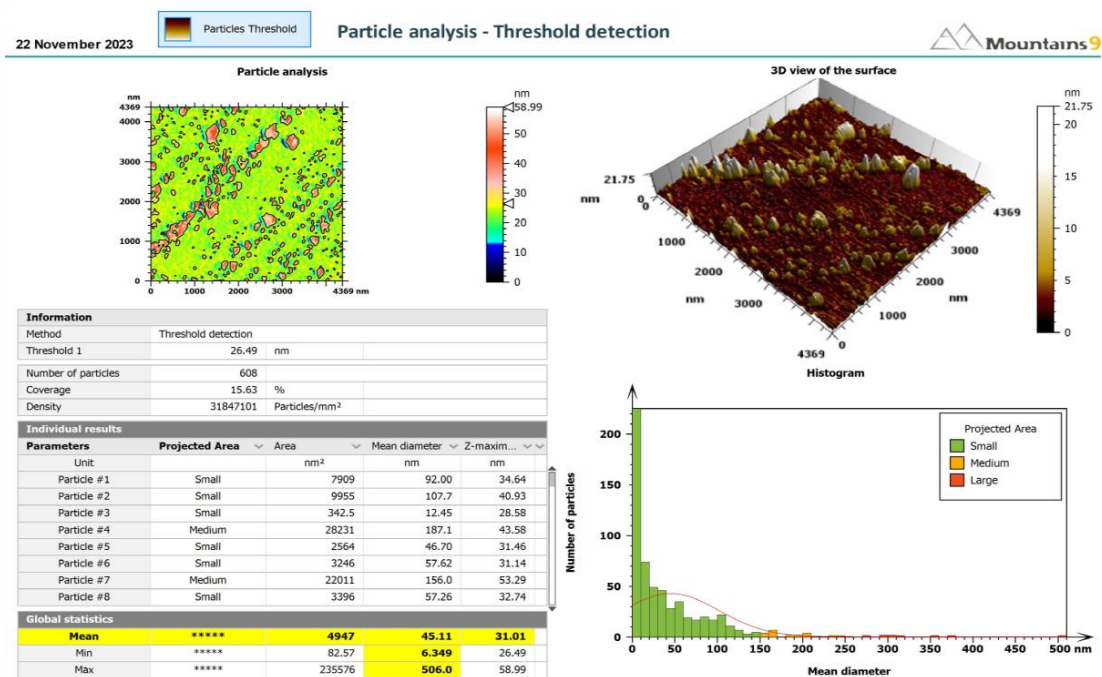


Figure 4. Particle analysis of ZrO₂ NPs

3.4 The XRD and EDX Analyses

Based on the X-ray diffraction (XRD) study presented in **Table 2** and **Figure 5**, it has been determined that the crystal planes of ZrO₂ nanoparticles, which are consistent with miller indices (101), (110), (200), (211), and (220), have been assigned to a series of diffraction peaks at 2θ values of 30.18, 34.98, 50.41, 59.95, and 74.29, respectively, belonging to the JCPDS card number (79-1769). The equation developed by Debye and Scherres was employed in order to determine the average crystal size ;

$D = 0.9 \lambda / \beta \cos \theta$, where D= the average crystalline size, the Cu K X-ray radiation ($\lambda = 1.5418 \text{ \AA}$), and it was equivalent to 7.21nm (Al-Saadi, 2022; Peng *et al.*, 2022).

Table 2. The XRD details for ZrO₂ NPs.

[°2Th.]	Height [cts]	FWHM [°2Th.]	Particle size (nm)	Average crystal size (nm)
30.18	947	0.95	9.05	
34.98	185	1.12	7.77	
50.41	536	1.09	8.42	7.65
59.95	328	1.33	7.21	
74.29	43	1.8	5.79	

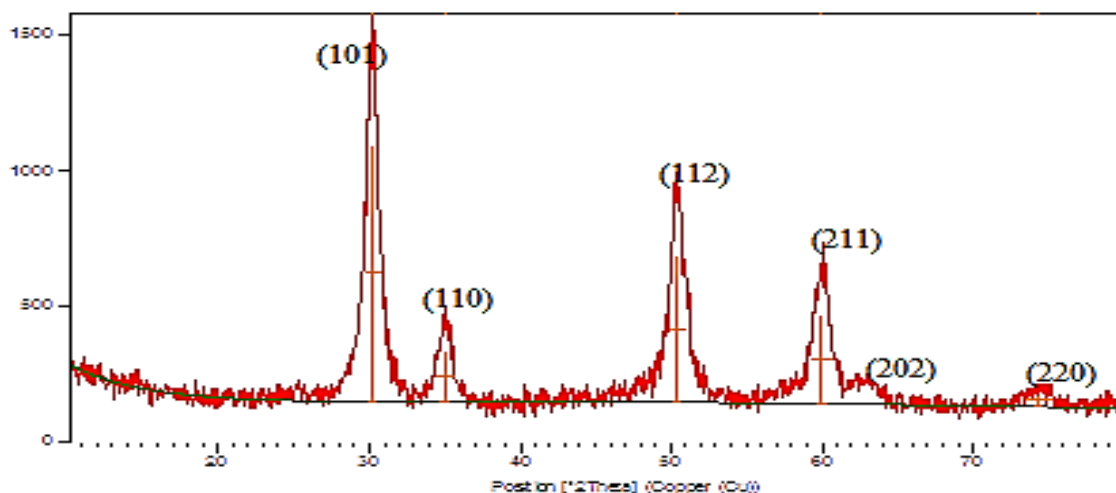


Figure 5. The XRD pattern of ZrO₂ NPs

EDX was used to analyze the percentage of elements in the sample, and the results obtained from this analysis revealed a characteristic peak associated with the % element composition (Zr and O), which corresponds to the exact composition of the sample under study as shown in **Figure 6**. The element percentages showed 69.10% for zirconium and 30.90% for oxygen (Ali and Ewies, 2023; Ramos-Justicia *et al.*, 2023; Sagadevan *et al.* 2016)

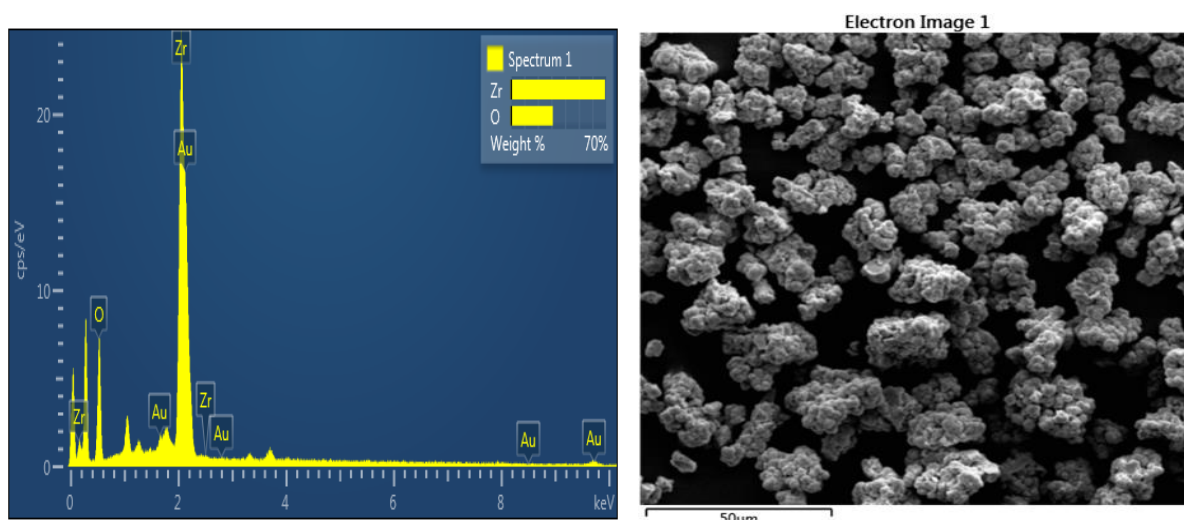


Figure 6. The EDX of ZrO₂ NPs

3.5 SEM analyses

The morphology and structure of the nanomaterial were determined by scanning electron microscopy. The SEM analyzes, were performed due to the presence of a limited amount of morphology ZrO₂ NPs with nanostructured morphology, This can be seen from the shapes of the SEM images in **Figure 7**, and the size of the diameters ZrO₂ NPs about 18.70 nm, and this confirms the precise formation of zirconium oxide nanoparticles using the Thyme plant ([Ahmed *et al.*, 2022](#); [Mohan and Shaalan, 2023](#))

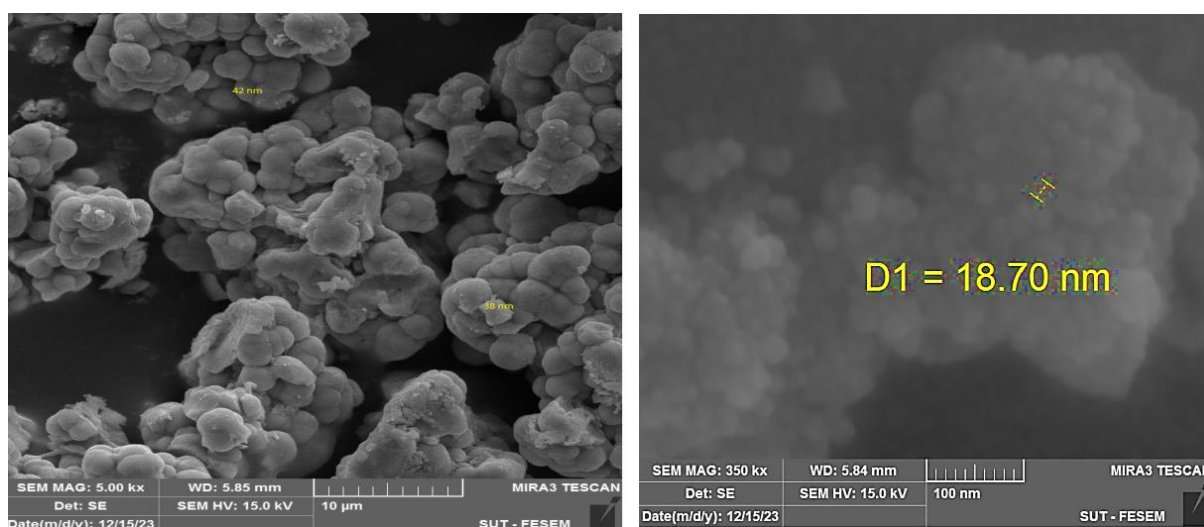


Figure 7. The images of SME for ZrO₂ NPs

3.6 Antimicrobials Activity

At concentrations of 25, 50, and 100% mg/L in DMSO solvent medium, the antibacterial activity of the synthesized ZrO₂ nanoparticles generated from Thyme plant extract was evaluated using the agar well diffusion method ([Naji, *et al.*, 2017](#); [Abdalsahib and Karem, 2023](#)). The results of this evaluation are depicted in **Figures 8 and 9**. *Bacillus*, *Klebsiella*, and *Candida fungus* were the organisms that were investigated. The antibiotics were tested on these bacteria and fungi, which served as controls. The ZrO₂ nanoparticles' antibacterial activity was evaluated by analyzing the inhibition zone of growth against the pathogens that were used. This was done after the nanoparticle concentration was changed on a number of occasions.

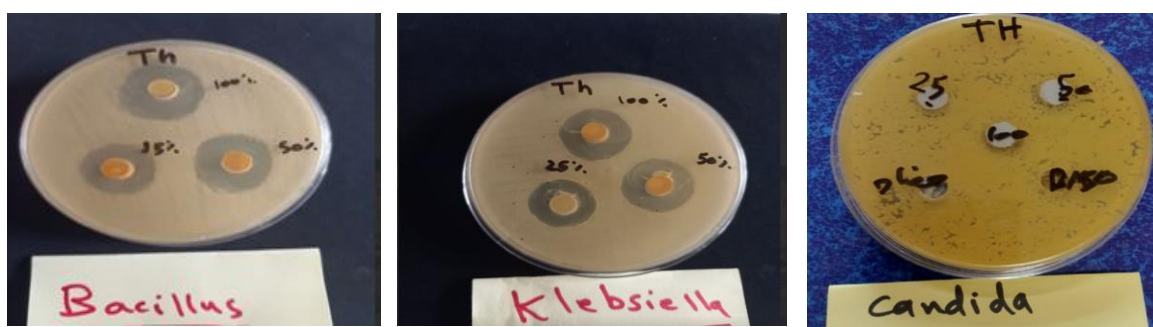


Figure 8. The Antibacterial activity of ZrO₂ NPs from Thyme plant extract

According to the findings, that good inhibition is obtained against the two different species of bacteria at all three concentrations, but that low inhibition is obtained against fungus at the 25% concentration when compared to the other concentrations. The result due to that the antimicrobial activity of metal nanoparticles on bacteria was dependent on the concentration of metal nanoparticles and was closely associated with the formation of pits in the cell wall of bacteria thus interfering with the ability of bacteria to continually form cell walls hence causing the cell wall to disintegrate. Some other important factors such as nature of the metal ion, metal ion coordinating site, hydrophobicity and presence of co-ligands have considerable influence on the antibacterial activity (Mahmoud, *et al.*, 2020; Uddin, *et al.*, 2020). Therefore, the antibacterial activity of the metal oxide cannot be ascribed to chelation alone but it's an intricate blend of all of the above contributions.

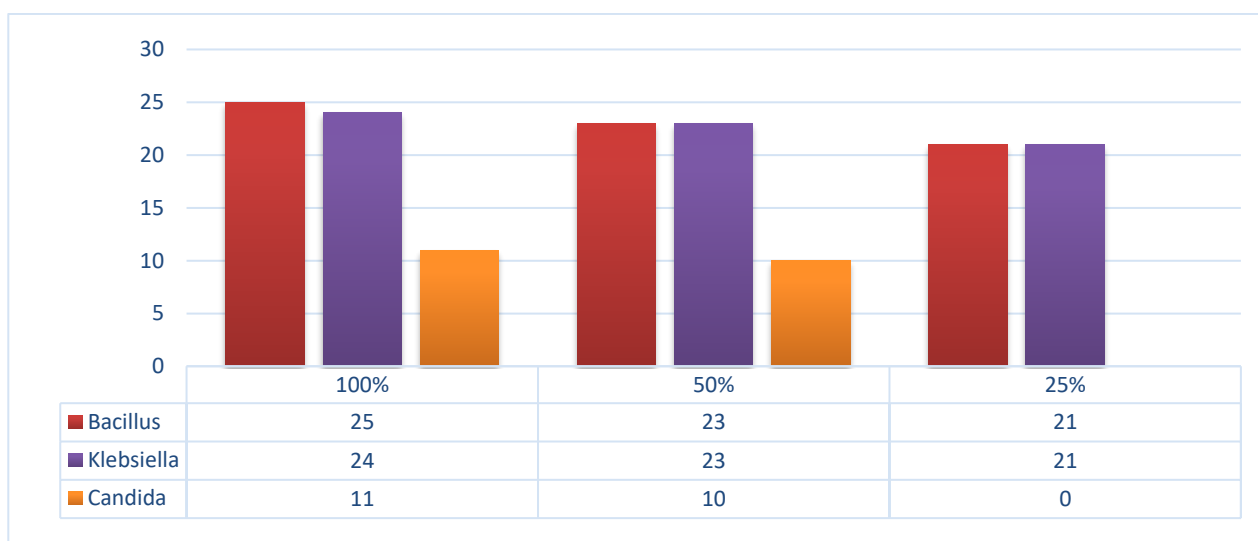


Figure 9. The Antibacterial activity of ZrO₂ NPs from Thyme Plant Extract

3.6 Anticancer Assay Study

We tested MCF-7 cell lines with ZrO₂ NPs in concentration (15.625, 31.25, 62.5, 125, 250 and 500) µg/mL with doxorubicin as control to see how well they inhibited the development of cancer. As the quantities of ZrO₂ NPs and doxorubicin increased, cell viability as demonstrated in **Table 3** and **Figure 10**. ZrO₂ NPs, when tested against MCF-7 at a concentration of (500 µg/mL) showed the viability was 66.70. The lower IC₅₀ value 21.35 µg/mL it is the concentration value when the inhibition is at the value 84.86, was see in **Figure 11**. the microscopic pictures displayed in **Figure 12**, The unique physical and chemical properties, namely tiny size, high specific surface area, and high reactivity, caused this impact to be dose-dependent (Abdel-Tawab, 2021; Majeed *et al.*, 2021).

Table 3. Inhibition (%) of ZrO₂ NPs and Standard Drug against MCF-7 Cell Lines

Concentrations($\mu\text{g/ml}$)	500	250	125	62.5	31.25	15.625	Control
	0.146548	0.162513	0.191028	0.220533	0.214726	0.238654	0.213426
	0.147727	0.181131	0.210281	0.223104	0.252643	0.205851	0.218997
	0.125679	0.187506	0.172242	0.181965	0.204696	0.239962	0.224882
	0.144629	0.189847	0.217953	0.208799	0.238665	0.214517	0.247339
	0.157978	0.175674	0.1636	0.217923	0.240956	0.24102	0.216051
	0.171835	0.183929	0.188041	0.195177	0.229746	0.196386	0.220098
Mean	0.149066	0.1801	0.190524	0.207917	0.230238	0.222732	0.223466
standard deviation	0.015314	0.009944	0.021016	0.016288	0.017783	0.019654	0.012321
Viability	66.70643	80.59411	85.25892	93.04208	103.0308	99.67156	100
Stdev.v	6.853082	4.450018	9.404409	7.28896	7.957713	8.795137	5.513506

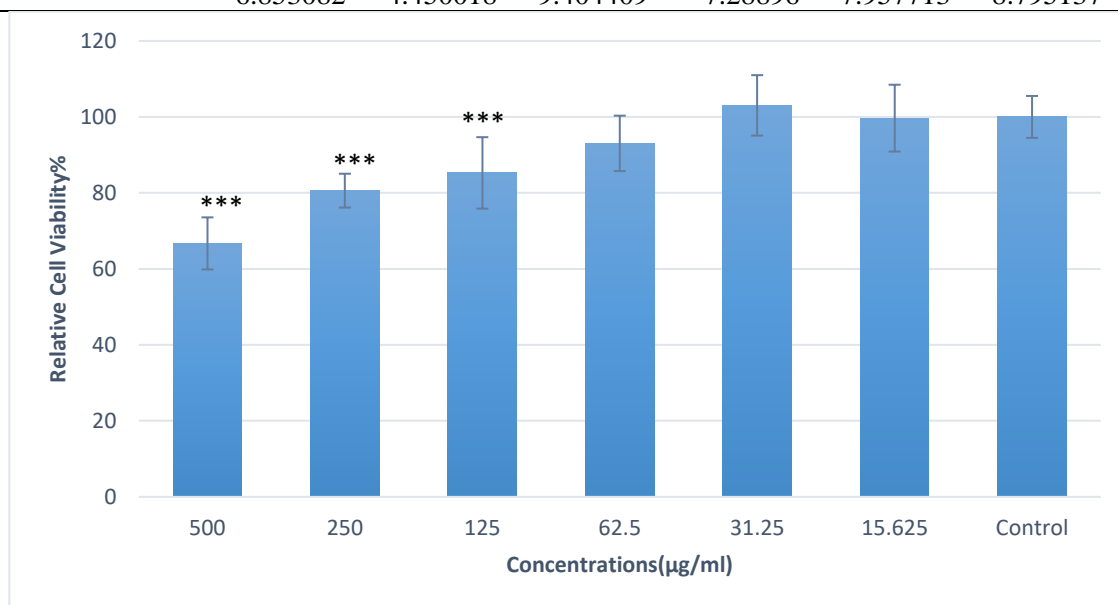


Figure 10. The Cytotoxicity for ZrO₂ NPs against MCF-7 cell lines

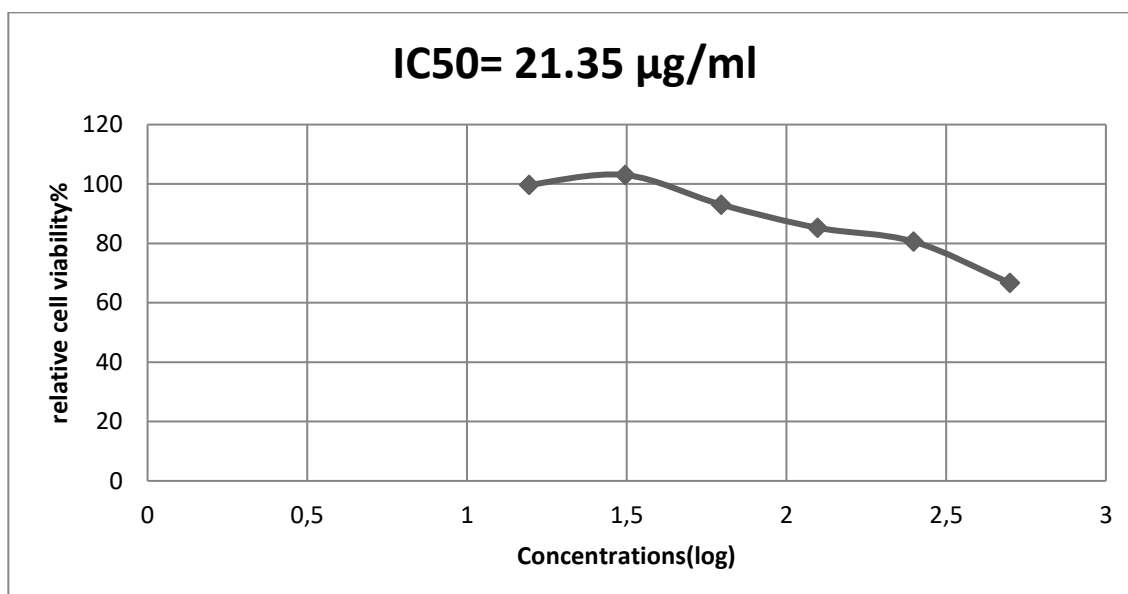


Figure 11. The ZrO₂ NPs of IC₅₀ (21.35 $\mu\text{g/ml}$)

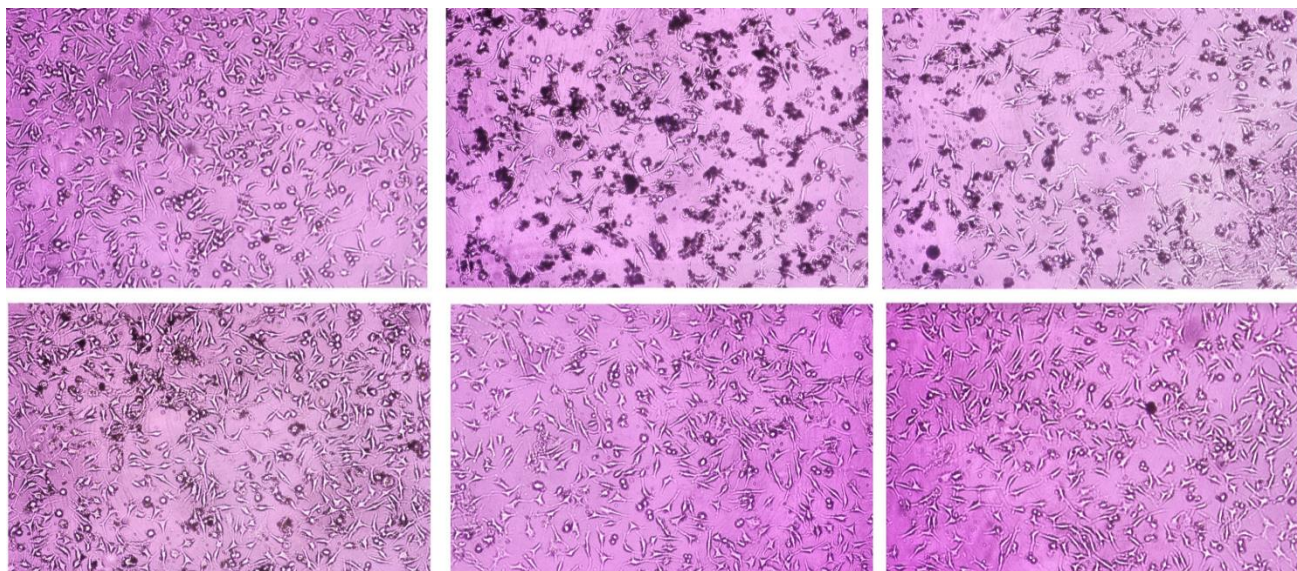


Figure 12. The cancer cell treated with ZrO₂ NPs

Conclusion

This research describes a green synthesis of ZrO₂ NPs using an extract from the thyme plant, which is both efficient and environmentally benign. Due to the existence of a limited amount of morphology, ZrO₂ NPs were diagnosed using FTIR, UV visible, Atomic force microscope results showed the typical size values for ZrO₂ NPs were 45.11 nm, and there are several distortions due to the presence of some large sizes. SEM techniques was used to provide information about the surface topography and composition of the sample, the results of SEM show that values size of particles ZrO₂ NPs was 18.70 nm, zirconium oxide nanoparticles are formed in small clusters. The XRD technique was used to determine the average crystal size of the ZrO₂ NPs, which is 7.65 nm, and the EDX analysis verified the presence of the element ratios, which demonstrated 69.10% zirconium and 30.90% oxygen. The particles are small and spherical. The efficacy of Nano zirconium oxide against various antimicrobials was found to vary. Microscopic examination with extremely low cell density validated the anticancer efficacy of the ZrO₂ NPs cell line, and the nanoparticles exhibited a strong inhibitory effect (66.70) with a modest IC₅₀ value of 21.35 µg/mL.

Acknowledgement: The authors of this paper would like to express their sincere gratitude to the chemistry department of Ibn-Al Haitham University of Baghdad, Iraq for providing financial support for this article.

Disclosure statement: *Conflict of Interest:* The authors declare that there are no conflicts of interest.

Compliance with Ethical Standards: This article does not contain any studies involving human or animal subjects.

References

- A Aaddouz, M., Azzaoui, K., Akartasse, N., Mejdoubi, E., *et al.* (2023) Removal of methylene blue from aqueous solution by adsorption onto hydroxyapatite nanoparticles, *Journal of Molecular Structure*, 1288(15), 135807. <https://doi.org/10.1016/j.molstruc.2023.135807>.
- Abdalsahib, N.M. and Karem, L.K.A. (2023) Preparation, Characterization, Antioxidant and Antibacterial Studies of New Metal (II) Complexes with Schiff Base for 3-amino-1-phenyl-2-pyrazoline-5-one, *International Journal of Drug Delivery Technology*, 13(1), 290–296. DOI: 10.25258/ijddt.13.1.47
- Abdalsahib, N.M. and Karem, L.K.A. (2023) Synthesis, Characterization, Antioxidant and Antibacterial Studies for New Schiff Base Complexes derived from 4-Bromo-O-toluidine, *International Journal of Drug Delivery Technology*, 13(2), 679-685. DOI: 10.25258/ijddt.13.2.33

- Abdel-Tawab M. (2021) Considerations to be taken when carrying out medicinal plant research—what we learn from an insight into the IC50 values, bioavailability and clinical efficacy of exemplary anti-inflammatory herbal components, *Pharmaceuticals*, 14(5), 437. doi.org/10.1016/j.matlet.2019.127255
- Akartasse, N., Azzaoui, K., Mejdoubi, E., Lhaj Lahcen Elansari, et al. (2022) Chitosan-Hydroxyapatite BioBased Composite in Film Form: Synthesis and Application in Wastewater, *Polymers*, 14(20), 4265. <https://doi.org/10.3390/polym14204265>
- Alexa, E., et al (2018) Synergistic antifungal, allelopathic and anti-proliferative potential of *Salvia officinalis* L., and *Thymus vulgaris* L. essential oils. *Molecules*, 23(1), 185. doi.org/10.3390/molecules23010185
- Al-Menhali, Afnan, et al (2015) *Thymus vulgaris* (thyme) inhibits proliferation, adhesion, migration, and invasion of human colorectal cancer cells, *Journal of medicinal food*, 18(1) , 54-59. <https://doi.org/10.1089/jmf.2013.3121>.
- Azadi, M., Moghaddam S.S., Rahimi A., Pourakbar L., Popović-Djordjević J. (2021) Biosynthesized silver nanoparticles ameliorate yield, leaf photosynthetic pigments, and essential oil composition of garden thyme (*Thymus vulgaris* L.) exposed to UV-B stress, *Journal of Environmental Chemical Engineering*, 9(5) ,105919.
- Azzaoui, K.; Mejdoubi, E; Lamhamdi, A; et al. (2016) Novel tricomponenets composites films from polylactic acid/ hydroxyapatite/ poly-caprolactone suitable for biomedical applications, *Journal of Materials and Environmental Science*. 7(3), 761 – 769.
- Azzaoui K., Aaddouz M., et al. (2023) Synthesis of β -Tricalcium Phosphate/PEG6000 Composite by Novel Dissolution/Precipitation Method: Optimization of the Adsorption Process Using a Factorial Design-DFT and Molecular Dynamic. *Arab. J. Sci. Eng.* 49, 711–732. <https://doi.org/10.1007/s13369-023-08390-8>.
- Azzaoui K., Lamhamdi A., Mejdoubi E., Hammouti B., Berrabah M. (2014) Synthesis of hydroxyethylcellulose and hydroxyapatite nanocomposite for analysis of bisphenol, *Arabian Journal of Chemical and Environmental Research*. 1(1), 41–48.
- Ahmed, A., Majeed I. Y., Asaad N. et al. (2022) Some 3, 4, 5-trisubstituted-1, 2, 4-triazole synthesis, antimicrobial activity, and molecular docking studies, *Egyptian Journal of Chemistry*, 65(3), 395–401. <https://doi.org/10.21608/ejchem.2021.93025.4397>
- Al-Bahadili, Z.R., AL-Hamdani A.A.S., Rashid F.A., et al. (2022) An Evaluation of the Activity of Prepared Zinc Nanoparticles with Extracted Alfalfa Plant in the Treatment of Heavy Metals, *Baghdad Science Journal*, 19(6 (Suppl.)), 1399. <https://doi.org/10.21123/bsj.2022.7313>.
- Al-Saadi, T.M. (2022) Investigating the Structural and Magnetic Properties of Nickel Oxide Nanoparticles Prepared by Precipitation Method, *Ibn Al-Haitham Journal For Pure and Applied Sciences*, 35(4), 94–103. <https://doi.org/10.30526/35.4.2872>.
- Al-Saadi, T.M. and Kamil, Z.A. (2023) Study the Effect of Manganese Ion Doping on the Size-Strain of SnO₂ nanoparticles Using X-Ray Diffraction Data, *Ibn AL-Haitham Journal For Pure and Applied Sciences*, 36(3), 158–166. <https://doi.org/10.30526/36.3.3052>.
- Ali, A.T. and Ewies, E.F. (2023) Biosynthesis, Characterization, Adsorption and Antimicrobial Studies of Zirconium Oxide Nanoparticles Using *Punica Granatum* Extract, *Ibn AL-Haitham Journal For Pure and Applied Sciences*, 36(4), 262–273. <https://doi.org/10.30526/36.4.3167>.
- Aliyu, A.O., Garba, S. and Bognet, O. (2017) Green synthesis, characterization and antimicrobial activity of vanadium nanoparticles using leaf extract of *Moringa oleifera*, *International Journal of Chemical Sciences*, 16(1), 231.
- Al Jabbar, J.L., Apriandanu D. O. B., Yulizar Y. et al. (2020) Synthesis, characterisation and catalytic activity of V₂O₅ nanoparticles using *Foeniculum vulgare* stem extract, *IOP Conference Series: Materials Science and Engineering*, 763, 12031. <https://doi.org/10.1088/1757-899X/763/1/012031>
- Alsahib, S.A. (2020) Characterization and biological activity of some new derivatives derived from sulfamethoxazole compound, *Baghdad Sci. J.*, 17(2), 471–480. <https://doi.org/10.21123/bsj.2020.17.2.0471>.
- Amer, A.A. and Karem, L.K.A. (2022) Biological Evaluation and Antioxidant Studies of Nio, Pdo and Pt Nanoparticles Synthesized from a New Schiff Base Complexes, *Ibn AL-Haitham Journal For Pure and Applied Sciences*, 35(4), 170–182. <https://doi.org/10.30526/35.4.2864>.
- Amer, A.A. and Karem, L.K.A. (2023) Synthesis, Characterization, Antimicrobial and Antioxidant Study of New Complexes Schiff Base Derived from 2, 5-diChloroaniline, *International Journal of Drug Delivery Technology*, 13(2), 686-691. DOI: 10.25258/ijddt.13.2.34.

- Balasooriya, E.R., Jayasinghe C. D., Jayawardena U. A., *et al.* (2017) Honey mediated green synthesis of nanoparticles: new era of safe nanotechnology, *Journal of Nanomaterials*, 2017, Article ID 5919836. <https://doi.org/10.1155/2017/5919836>.
- Bukhari, A., Ijaz, I., Gilani, E. *et al.* (2021) Green synthesis of metal and metal oxide nanoparticles using different plants' parts for antimicrobial activity and anticancer activity: a review article, *Coatings*, 11(11), 1374. <https://doi.org/10.3390/coatings11111374>
- Carreño, E.A., Alberto, A.V.P., de Souza, C.A.M., *et al.* (2021) Considerations and technical pitfalls in the employment of the MTT assay to evaluate photosensitizers for photodynamic therapy, *Applied Sciences*, 11(6), 2603. <https://doi.org/10.3390/app11062603>
- Diniz, M.O., Golin A.F., Santos M.C. *et al.* (2019) Improving performance of polymer-based ammonia gas sensor using POMA/V₂O₅ hybrid films, *Organic Electronics*, 67, 215–221. <https://doi.org/10.1016/j.orgel.2019.01.039>.
- Ebrahimian, J., Mohsennia, M. and Khayatkashani, M. (2020) Photocatalytic-degradation of organic dye and removal of heavy metal ions using synthesized SnO₂ nanoparticles by Vitex agnus-castus fruit via a green route, *Materials Letters*, 263, 127255. <https://doi.org/10.1016/j.matlet.2019.127255>.
- Ghani, S., Rafiee B., Bahrami S., *et al.* (2022) Green synthesis of silver nanoparticles using the plant extracts of vitex agnus castus L: An ecofriendly approach to overcome antibiotic resistance, *International Journal of Preventive Medicine*, 13,133. [10.4103/ijpvm.ijpvm_140_22](https://doi.org/10.4103/ijpvm.ijpvm_140_22)
- Gonzalez-Rodriguez, J.G., Gutierrez-Granda, D.G., Larios-Galvez, A.K. *et al.* (2022) Use of Thymus vulgaris Extract as Green Corrosion Inhibitor for Bronze in Acid Rain. *J. Bio. Tribo. Corros.* 8, 77. <https://doi.org/10.1007/s40735-022-00676-y>
- Hamdouch, A., Anejjar A., Bijla L., *et al.* (2023) Corrosion inhibition of carbon steel by Vitex agnus castus leaves essential oils from the oasis of Tata, *Moroccan Journal of Chemistry*, 11(1), 105-118. <https://doi.org/10.48317/IMIST.PRSM/morjchem-v11i1.37301>
- Hameed, H.G. and Abdulrahman, N.A. (2023) Preparation and Characterization of TiO₂ Nanoparticles With and Without Magnetic Field Effect Via Hydrothermal Technique, *Iraqi Journal of Science*, 3225–3231. <https://doi.org/10.24996/ijs.2023.64.7.3>.
- Herradi, S., Zerrouk M., Bouayad A. *et al.* (2024) Removal of methylene blue with a highly effective hydroxyapatite-silica nanocomposite, *Moroccan Journal of Chemistry*, 12(1), 267-285. <https://doi.org/10.48317/IMIST.PRSM/morjchem-v12i1.44168>.
- Horváth, G., Horváth, A., Reichert, G. *et al.* (2021) Three chemotypes of thyme (*Thymus vulgaris* L.) essential oil and their main compounds affect differently the IL-6 and TNF α cytokine secretions of BV-2 microglia by modulating the NF- κ B and C/EBP β signalling pathways. *BMC Complement Med Ther* 21, 148. <https://doi.org/10.1186/s12906-021-03319-w>
- Hosseinzadeh, Saleh, *et al.* (2015) The application of medicinal plants in traditional and modern medicine: a review of *Thymus vulgaris*. *International Journal of Clinical Medicine*, 6(09), 635-642. [doi:10.4236/ijcm.2015.69084](https://doi.org/10.4236/ijcm.2015.69084).
- Karem, L.K.A. and Ali, A.T. (2023) Biosynthesis, characterization, adsorption and antimicrobial studies of vanadium oxide nanoparticles using *Punica granatum* extract, *Baghdad Science Journal*, 21(2), 410-421. <https://doi.org/10.21123/bsj.2023.8114>.
- Khan, S., Mansoor S., Rafi Z. *et al.* (2022) A review on nanotechnology: Properties, applications, and mechanistic insights of cellular uptake mechanisms, *Journal of Molecular Liquids*, 348(9), 118008. <https://doi.org/10.1016/j.molliq.2021.118008>
- Mahdi, S.H. and Karem, L.K.A. (2020) Synthesis, Physicochemical Studies and biological estimation of new mixed ligand complexes from heterocyclic compounds, *International Journal of Pharmaceutical Research*, Supplementary Issue 1, 1734-1740. <https://doi.org/10.31838/ijpr/2020>
- Mahmoud, W.H., Deghadi, R.G., Mohamed, G.G. (2020) Metal complexes of ferrocenyl-substituted Schiff base: Preparation, characterization, molecular structure, molecular docking studies, and biological investigation, *J. Organomet. Chem.*, 917, 121113. doi.org/10.1016/j.jorganchem.2020.121113.
- Maizia R., Zaabar A., Djermoune A., Amoura D., Martemianov S., Thomas A., Alrashdi A.A., Makhloufi L., Lgaz H., Dib A., Chafiq M., Ko Y. G. (2023), Experimental assessment and molecular-level exploration of the mechanism of action of Nettle (*Urtica dioica* L.) plant extract as an eco-friendly corrosion inhibitor for X38 mild steel in sulfuric acidic medium, *Arabian Journal of Chemistry*, 16(8), 104988, <https://doi.org/10.1016/j.arabjc.2023.104988>

- Majeed, I.Y., Ahmed A., Ahmed R.M. *et al.* (2021) Comparison among the Synthesis of Some Azomethine Derivatives by Classical and Non-classical Methods, *International Journal of Drug Delivery Technology*, 11(2), 515-517. DOI: 10.25258/ijddt.11.2.49.
- Mohan, B. and Shaalan, N. (2023) Synthesis, Spectroscopic, and Biological Activity Study for New Complexes of Some Metal Ions with Schiff Bases Derived From 2-Hydroxy Naphthaldehyde with 2-amine benzhydrazide, *Ibn AL-Haitham Journal For Pure and Applied Sciences*, 36(1), 208–224. <https://doi.org/10.30526/36.1.2978>.
- Naji, S.H., Karim, L.K.A. and Mousa, F.H. (2013) Synthesis, Spectroscopic and Biological Studies of a New Some Complexes with N-Pyridin-2-Ylmethyl-Benzene-1, 2Diamine, *Ibn AL-Haitham Journal For Pure and Applied Science*, 26(1), 193–207. <https://jih.uobaghdad.edu.iq/index.php/j/article/view/525>.
- Peng, J., Guo J., Ma R. *et al.* (2022) Water-solid interfaces probed by high-resolution atomic force microscopy', *Surface Science Reports*, 77(1), 100549. <https://doi.org/10.1016/j.surfrep.2021.100549>.
- Proks, M., Heghes, A., Cheveresan, A., Nita, S., Voicu, M., Buda, V., Ionescu, D., Nita, L., Trandafirescu, C., Paunescu, V. (2019), Thyme Leaves Aqueous Extract and its Formulations. A comparative study based on chemical structures and biological activity, *Rev. Chim.*, 70(5), 1875-1878. <https://doi.org/10.37358/RC.19.5.7236>
- Qiu, L., Zhu N., Feng Y. *et al.* (2020) A review of recent advances in thermophysical properties at the nanoscale: From solid state to colloids, *Physics Reports*, 843, 1–81. <https://doi.org/10.1016/j.physrep.2019.12.001>.
- Ramos-Justicia J.F., Ballester-Andújar J.L., Urbietta A., Fernández P. (2023) Growth of Zr/ZrO₂ Core-Shell Structures by Fast Thermal Oxidation. *Applied Sciences*, 13(6), 3714. doi.org/10.3390/app13063714
- Ruaa, M.D., Alsaheb, S.A. and Ascar, I.F. (2021) Synthesis, characterization and cyclization of pyran using Ag₂O nanoparticle from natural source “Ginger”, *Iraqi Journal of Agricultural Sciences*, 52(5), 1171–1184. <https://doi.org/10.36103/ijas.v52i5.1455>.
- Sagadevan S., Podder J., Das I. (2016) Hydrothermal synthesis of zirconium oxide nanoparticles and its characterization. *J. Mater. Sci: Mater. Electron.* 27, 5622–5627. <https://doi.org/10.1007/s10854-016-4469-6>
- Salem, S.S., Hammad E.N., Mohamed A.A. *et al.* (2022) A comprehensive review of nanomaterials: Types, synthesis, characterization, and applications, *Biointerface Res. Appl. Chem*, 13(1), 41. <https://doi.org/10.33263/BRIAC131.041>
- Salem S.S. and Fouda, A. (2021) Green synthesis of metallic nanoparticles and their prospective biotechnological applications: an overview, *Biological Trace Element Research*, 199, 344–370. <https://doi.org/10.1007/s12011-020-02138-3>
- Shvets P., Dikaya O. *et al.* (2019) A review of Raman spectroscopy of vanadium oxides, *Journal of Raman spectroscopy*, 50(8), 1226–1244. <https://doi.org/10.1002/jrs.5616>
- Singh R. and Singh S. (2019) Nanomanipulation of consumer goods: effects on human health and environment, *Nanotechnology in Modern Animal Biotechnology: Recent Trends and Future Perspectives*, 221–254. https://doi.org/10.1007/978-981-13-6004-6_7
- Subramanian M., Dhayabaran V.V., Shanmugavadivel M. (2019) Room temperature fiber optic gas sensor technology based on nanocrystalline Ba₃(VO₄)₂: Design, spectral and surface science, *Materials Research Bulletin*, 119, 110560. <https://doi.org/10.1016/j.materresbull.2019.110560>.
- Tabaght F. E., Azzaoui K., *et al.* (2021) New nanostructure based on hydroxyapatite modified cellulose for bone substitute, synthesis, and characterization, *International Journal of Polymeric Materials and Polymeric Biomaterials*, 70:6, 437-448. <https://doi.org/10.1080/00914037.2020.1725758>.
- Uddin M. N., Ahmed S. S., Alam S. M. R. (2020) Biomedical applications of Schiff base metal complexes, *Journal of Coordination Chemistry*, 73(23), 3109–3149. doi.org/10.1080/00958972.2020.1854745

(2024) ; <https://revues.imist.ma/index.php/morjchem/index>